



Detection of Landau band coupling induced rearrangement of the Hofstadter butterfly[☆]

M.C. Geisler^{a,*}, J.H. Smet^a, V. Umansky^b, K. von Klitzing^a, B. Naundorf^c,
R. Ketzmerick^d, H. Schweizer^e

^aMax-Planck-Institut für Festkörperforschung, Heisenbergstr. 1, D-70569 Stuttgart, Germany

^bBraun Center for Submicron Research, Weizmann Institut of Science, Rehovot 76100, Israel

^cMax-Planck-Institut für Strömungsforschung and Institut für Nichtlineare Dynamik der Universität Göttingen, Bunsenstr. 10, 37073 Göttingen, Germany

^dInstitut für Theoretische Physik, Technische Universität Dresden, 01062 Dresden, Germany

^eIV Physikalisches Institut, Universität Stuttgart, D-70550 Stuttgart, Germany

Available online 19 August 2004

Abstract

The spectrum of two-dimensional 2D electrons subjected to a weak 2D potential and a perpendicular magnetic field is composed of Landau bands with a fractal internal pattern of subbands and minigaps referred to as Hofstadter's butterfly. The Hall conductance may serve as a spectroscopic tool as each filled sub-band contributes a specific quantized value. Advances in sample fabrication now finally offer access to the regime away from the limiting case of a very weak potential. Complex behavior of the Hall conductance is observed and assigned to Landau band coupling induced rearrangements within the butterfly.

© 2004 M.C. Geisler. Published by Elsevier B.V. All rights reserved.

Keywords: Hofstadter butterfly; Quantum Hall effect; Superlattice; 2D electron gas

The intricate energy spectrum of two-dimensional (2D) electrons, simultaneously exposed to a perpendicular magnetic field B and a 2D periodic potential, has been theoretically addressed mainly in two limiting cases. Either the influence of a weak B -field on a strong tight-binding lattice

potential is investigated [1,2] or the influence of a weak modulation potential on a Landau quantized electron system [2,3] is treated as a small perturbation. The latter is of main interest here. For both cases, the allowed states are governed by a single parameter Φ/Φ_0 , where Φ is the magnetic flux per unit cell of the periodic potential and $\Phi_0 = h/e$ the flux quantum. When plotted with Φ/Φ_0 or Φ_0/Φ as abscissa for the respective limiting cases, these states form the appealing Hofstadter butterfly spectrum in Fig. 1(a). It exhibits fractal properties and emerges in a variety of contexts.

[☆]Reprinted with permission from the American Physical Society from M. Geisler, J.H. Smet, V. Umansky, K. von Klitzing, B. Naundorf, R. Ketzmerick, H. Schweizer, Phys. Rev. Lett. 92 (2004) 256801. © 2004 American Physical Society.

*Corresponding author. Fax: +49-711-689-1010.

E-mail address: m.geisler@fkf.mpg.de (M.C. Geisler).

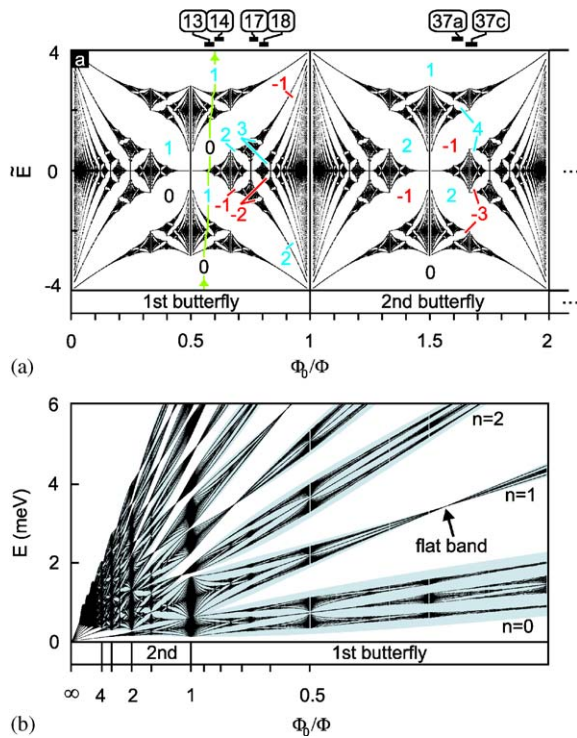


Fig. 1. (a) Repeated Hofstadter Butterfly. Hall conductance contributions in units of $\frac{2e^2}{h}$ of partially filled Landau bands are indicated in dominant gaps. The green line tracks the Fermi energy as Landau Band $n = 13$ is filled with decreasing flux. The resulting Hall sequence 0-1-0-1 can be identified. For other bands the Φ_0/Φ range is shown at the top. (b) Landau fan chart for modulation $V_0 = 2.4$ meV and period $a = 100$ nm in single band approximation. Weak 2D modulation subdivides blue Landau bands into repeated butterflies.

Fig. 1(b) displays the modifications to the discrete Landau level spectrum induced by a 2D periodic potential of the form $V(x, y) = V_0/4[\cos(2\pi x/a) + \cos(2\pi y/a)]$, if coupling among Landau levels is neglected. The modulation lifts the macroscopic degeneracy of each level and broadens them into bands with a B -dependent bandwidth. Furthermore, it produces internal structure to each Landau band. When Φ_0/Φ takes on a rational value of the form q/p , each band splits into p -subbands, which are q -fold degenerate and separated by minigaps. Here p and q are mutual primes. The band with orbital index $n = 0, 1, \dots$ is described by

$$E_n = \hbar\omega_c(n + \frac{1}{2}) + \frac{1}{8} V_0 \tilde{E} c^{-\frac{1}{2}} \pi \Phi_0/\Phi L_n(\pi \Phi_0/\Phi). \quad (1)$$

Here, $L_n(X)$ is the Laguerre polynomial of order n , $\hbar\omega_c$ is the cyclotron energy, \tilde{E} ranges from -4 to 4 and its allowed values for a certain Φ_0/Φ are precisely what the Hofstadter spectrum in Fig. 1(a) shows. This pattern of subbands and minigaps is identical for all bands and is repeated whenever Φ_0/Φ exceeds the next natural number. At the zeroes of $L_n(X)$, all subbands of Landau band n collapse on to each other. At this so-called flat band condition, the macroscopic degeneracy of the original Landau level is restored.

Gathering convincing evidence for this fractal spectrum has turned out a challenge. Hitherto only weak precursors for the most prominent of all minigaps in the left and right wing of the butterfly have been reported [3,4]. Significant progress was made by resorting to a long-standing prediction by Štředa and Thouless [5,6] or the behavior of the Hall conductance as the Fermi energy E_F is swept through the internal structure of a Landau band. In accordance with Laughlin's gauge invariance argument [7], the Hall conductivity is not only quantized in the Landau gaps, but also when E_F is located inside a minigap. The quantized contribution σ of such a partially filled band n to the total Hall conductance, σ_{xy} , varies from minigap to minigap in a non-trivial manner, but can easily be derived with a formula due to Štředa [5]. Selected minigaps have been labeled with their σ -values in units of $2e^2/h$ in Fig. 1(a). Whereas the longitudinal resistivity simply drops to zero, the quantized Hall conductance permits to distinguish between different minigaps and proves to be far more sensitive. The total Hall conductance will then be, $\sigma_{xy} = 2(\sigma + n)e^2/h$. The factor 2 accounts for spin degeneracy, as spin splitting is not resolved at the relevant fields. Higher-order butterflies emerge for $\Phi_0/\Phi > 1$ and keep the same subband structure, only the subband degeneracy increases with larger Φ_0/Φ . This leads to different σ -values for each butterfly, as seen in Fig. 1(a).

In this Paper, we report on significant advances in this field by exploiting the quantum Hall conductance as a diagnostic tool. On account of progress in the growth of high-quality shallow heterostructures and in the development of fabrication procedures for creating short period

lateral superlattices with minimal repercussions on the mobility, the Hall conductance now reveals higher order minigaps. What's more, these improvements disclose to experiment the so far unexplored regime in which Landau band coupling further enriches the physics. We present experimental evidence for Landau band coupling-induced rearrangements of minigaps and substantiate our interpretation with theoretical calculations.

The starting point is a shallow (100)-GaAs/AlGaAs heterostructure with the 2D electron gas buried 48 nm below the surface. A Hall-bar oriented along the [0 1 1]-direction is prepared (inset to Fig. 2) and covered with resist, patterned into a 102.7 nm square lattice of holes using e-beam lithography. A gate composed of 15 nm Cr and 95 nm Au is deposited on this pattern through a shadow mask with e-beam evaporation under a sequence of three angles while the sample is mounted on a liquid nitrogen cooled finger. Optimization of the evaporation process resulted in mobilities beyond 3.4×10^6 cm²/Vs after illumination with a red LED. A modulation strength of $V_0 \approx 1\% E_F$ is estimated from the positive magnetoresistance near zero field.¹ A voltage applied to the periodically displaced gate hardly affects V_0 . Instead, the gate acts as a grid of periodic stressors and induces a modulation via the non-zero piezoelectric effect along the {0 1 1}-directions of the GaAs crystal. Magnetoresistance measurements were carried out using standard lock-in techniques at approximately 50 mK. We were able to span the range of densities from $2.8\text{--}4.3 \times 10^{11}$ /cm² by combining gate voltage tuning with the virtues of the persistent photo-conductivity effect upon automated brief illuminations with red light. Even so, our main findings can be illustrated in the single B -field sweep trace of ρ_{xx} and ρ_{xy} at the fixed density $n_s = 4.32 \times 10^{11}$ cm⁻² shown in Fig. 2.

We briefly describe the strong B -field regime, where Landau bands are well separated, in order to establish the reliability of our procedures and illustrate the powerfulness of a Hall measurement

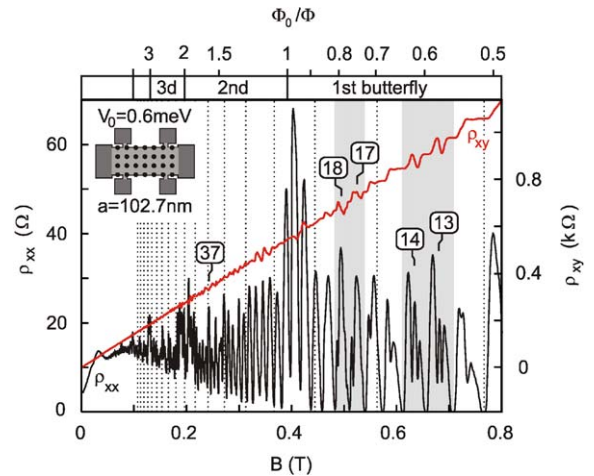


Fig. 2. Longitudinal and Hall resistivities for $n_s = 4.32 \times 10^{11}$ cm⁻². The modulation period is 102.7 ± 0.5 nm. Dotted lines mark flat band positions. The inset shows the sample geometry. Landau bands are denoted by their orbital index.

to unveil the internal Landau band structure. In the highlighted region of Fig. 2 between 0.6 and 0.7 T, Landau bands $n = 13$ and 14 are gradually populated as the B -field is lowered and E_F crosses the minigaps from the bottom to the top in the right wing of the first butterfly (Fig. 1) near $\Phi_0/\Phi = 0.6$. The Fermi energy does not trace a vertical line as Φ_0/Φ changes slightly upon lowering the field (for instance for band $n = 13$ from 0.56 to 0.6). It jumps abruptly in gapped regions, but otherwise moves towards larger Φ_0/Φ with a slope determined by the number of available states as seen for Landau band $n = 13$ in Fig. 1(a) (green line). Since these Landau bands are located far away from the flat band conditions, marked by dashed lines in Fig. 2, their internal gaps have non-zero width and the primary gaps that cause a three-fold splitting of the bands should be well resolved. When considering these gaps only, the contribution to the total Hall conductance is anticipated to vary non-monotonically as the Landau band is filled according to a 0-1-0-1 sequence (see green line in Fig. 1(a)). To compare with experiment, this sequence is plotted while taking the gap sizes of Fig. 1(a) as plateau widths (red trace in Fig. 3(a)). This curve is subsequently

¹P.H. Beton et al., Phys. Rev. B 42 (1990) 9229. The analysis is strictly valid only for one-dimensional (1D) modulation.

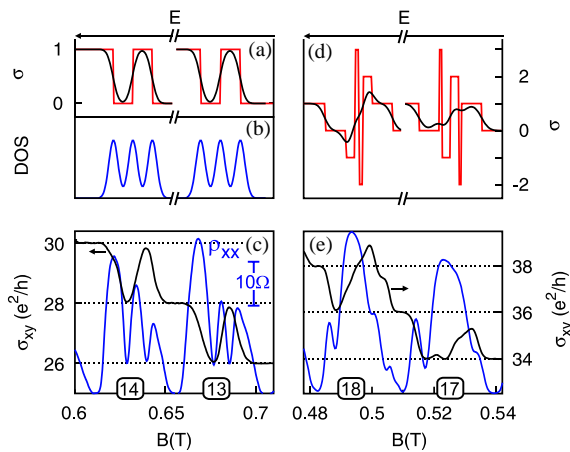


Fig. 3. (a) Expected Hall conductance for Landau bands $n = 13$ and 14 in red, obtained when taking the biggest gap sizes of Fig. 1(a) as plateau widths. Black lines are their convolution with a fitted Gaussian of width $0.013 \hbar\omega_c$. (b) Schematic representation of the density of states. (c) Measured Hall conductance (black) and longitudinal resistivity (blue) for bands $n = 13$ and 14 . (d) and (e) are like (a) and (c) but for bands $n = 17$ and 18 .

convoluted with a fitted Gaussian of width $0.013 \hbar\omega_c$ to simulate broadening (black trace in Fig. 3(a)).² The resulting non-monotonic behavior is already apparent in the Hall resistance measurement in Fig. 2. Fig. 3(c) displays a blown up version of the longitudinal resistivity as well as the Hall conductance, extracted from the inversion of the measured resistivity tensor. The Hall conductance nearly reaches the quantized values in accordance with the curve predicted from the heuristic procedure described above. This quantization is accompanied by deep dips in ρ_{xx} . Both observations attest to the unrivalled device quality.

Inspection of the fractal energy spectrum in Fig. 1 reveals that higher order minigaps of still sizeable but substantially reduced width open up at smaller B to both sides of $\Phi_0/\Phi = 0.8$. Landau bands $n = 17$ and 18 are the most suitable candidates to search for evidence of their existence as they are centered between the next pair of flat band conditions (see Fig. 2). The more complex

and distinct series of consecutive Hall conductance values when filling these bands are plotted in Fig. 3(d). Applying the same heuristic procedure reproduces all features including the weak shoulders and dents in Fig. 3(e). These fine features cannot be accounted for without invoking the much smaller minigaps with associated Hall conductances of $\sigma = 3$ and -2 . The ability to resolve such tiny minigaps in the Hofstadter spectrum is considered the crucial prerequisite, which was previously not satisfied, to investigate the intermediate field regime away from the limiting case of a very weak potential where Landau band coupling can no longer be ignored.

Continuing our journey along the horizontal axis of Fig. 2 towards smaller B -fields, we leave the first butterfly as Φ_0/Φ exceeds unity and more importantly enter this regime where single band calculations, which yield the spectrum in Fig. 1(a), no longer properly describe the experiment. Landau bands in Fig. 1(b) get closer for larger Φ_0/Φ and band coupling effects come into play. To avoid band crossings, the spectrum is distorted and some subbands rearrange. Hence, minigaps with unexpected Hall contributions emerge. Moreover, the spectrum is no longer universal and depends on the band index. This has been extensively investigated in theory for the 1st butterfly in Ref. [8], but experimental evidence remained elusive. The coupling strength can be captured by a single dimensionless parameter $K = 2\pi m^* a^2 V_0/h^2$, where $m^* = 0.067m_e$ is the effective mass of a conduction electron in GaAs. Here, K is of order 1 for the device at hand.

Fig. 4 illustrates how a Landau band calculation with neglected band coupling changes when coupling is switched on for band $n = 37$ and $K = 2$. Calculations along the lines of Ref. [8] were extended to handle the six nearest neighboring bands and to encompass Landau levels with far higher orbital indices as well as the 2nd butterfly for which, as opposed to the 1st butterfly, small coupling values K already produce significant effects. Not surprisingly, coupling has the strongest impact near the flat band locations of the uncoupled case. The macroscopic degeneracy is lifted and, in comparison with the $K = 0$ case, minigaps with unexpected Hall conductance values

²A theoretical treatment of the dirty Hofstadter butterfly is available only for the tight binding limit but not applicable here: H Aoki, Surf. Sci. 263 (1992) 137.

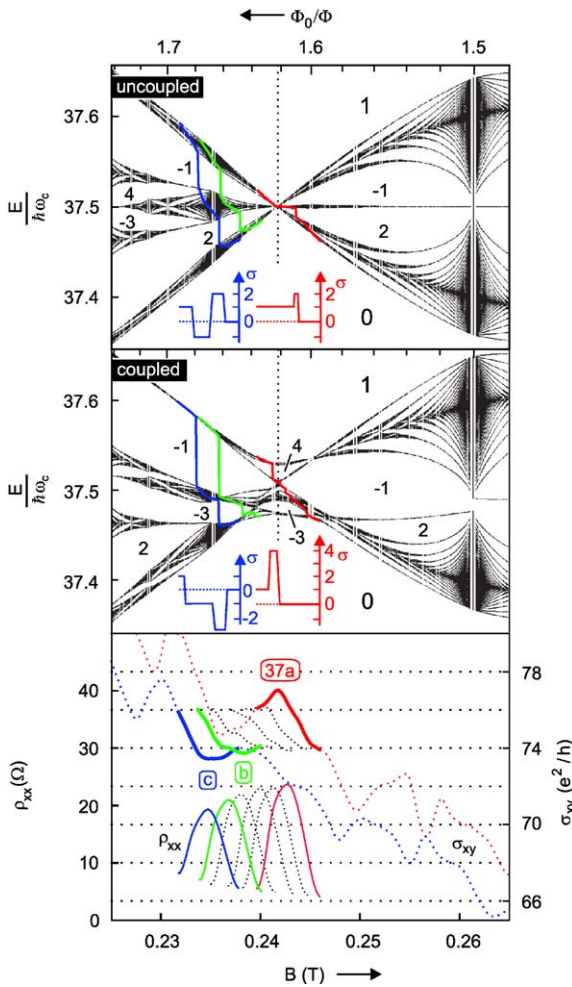


Fig. 4. Consequences of Landau band coupling: Top: Calculation of band $n = 37$ and $K = 2$ ignoring coupling with other bands. Hall conductances for major gaps are marked. Middle: Deformations due to coupling. As in the top panel, E_F traces are plotted for three densities. Jumps of E_F across gaps produce Hall plateaus. The expected Hall conductivity behavior is shown in the red and blue insets. Bottom: Measured Hall conductivity for n_s from $4.32 \times 10^{11} \text{ cm}^{-2}$ for **a** to $4.17 \times 10^{11} \text{ cm}^{-2}$ for **c**. Here, ρ_{xx} shows the boundary of the 37th band for each Hall trace.

appear. For the relatively small value of K , distortions persist further away from the original zero band width regions, yet no rearrangements occur. Worth mentioning is only the opening of the gap between the so-called kissing bands at $\Phi_0/\Phi = 1.5$. However, this phenomenon is not

suited for experimental verification of band coupling, due to the rapid variation of the energy spectrum in this region and hence its sensitivity to broadening and small changes in Φ_0/Φ . Putting it all together, at small K -values, only the flat band regions in higher order butterflies provide appropriate experimental windows to search for signatures of Landau band coupling. This motivates and justifies our choice of the 37th Landau band situated right at a flat band condition in the 2nd butterfly (see Fig. 2). The bottom panel of Fig. 4 displays the Hall conductivity for several carrier densities. For the sake of clarity, the Shubnikov–de Haas peaks have been added. They demarcate the field interval across which the 37th level is filled for the respective carrier density. We reiterate that the top panels are only valid for these sections of the Hall conductivity curves related to band $n = 37$. For selected values of n_s , the calculated behavior of the Fermi energy has been included in the top two panels. First focus on the red curve for the highest carrier density as the magnetic field is lowered (corresponding to the resistivity measurements plotted in Fig. 2). In the single band approximation (top panel in Fig. 4) the Fermi energy crosses a gap with $\sigma = 2$ during the *initial* stage of filling this band. This contradicts the experimental data, which shows an overshoot during the second half of populating the band. Instead, it fits to the numerical data with Landau band coupling (middle panel), where the Fermi energy passes a $\sigma = 4$ -gap when the band has been filled more than half. The small size of the gap unfortunately prevents the Hall conductivity from reaching its quantized value. Note that the Shubnikov–de Haas peak is featureless. This emphasizes once more that the Hall conductivity is a superior tool to study the fractal energy spectrum and excels in providing detailed information. The data at lower carrier densities further corroborate beyond doubt that Landau band coupling plays a dominant role. As an outcome of band interaction, the large gap with $\sigma = 2$ has closed and a gap with $\sigma = -3$ has taken its place. The consequences of this rearrangement for the Hall conductivity are depicted schematically in the blue insets of Fig. 4. For both curves **b** and **c**, the Hall conductivity drops ‘negative’ instantly as

the band is being filled. Curve **b** even develops its absolute minimum as the Fermi energy reaches the first significant gap in the spectrum. Neither of these observations can be reconciled with the positive contribution to the Hall conductance of $\sigma = 2$ predicted by the single band approximation.

In conclusion, due to significant advances in sample quality and fabrication, it is now possible to resolve higher order minigaps in Hofstadter's energy spectrum with recourse to the quantum Hall effect as a diagnostic tool. This progress has offered experimental access to the hitherto-unexplored regime where Landau band coupling further enriches the physics of this model problem with fractal nature.

The authors thank R. Gerhardts and C. Albrecht for fruitful discussions, as well as H. Gräbeldinger, T. Reindl and M. Riek for

technical assistance. This work has been supported by the GIF and the BMBF.

References

- [1] D. Hofstadter, *Phys. Rev. B* 14 (1976) 2239.
- [2] D. Langbein, *Phys. Rev.* 180 (1969) 633.
- [3] D. Pfannkuche, R. Gerhardts, *Phys. Rev. B* 46 (1992) 12606;
T. Schlösser, K. Ensslin, J.P. Kotthaus, M. Holland, *Europhys. Lett.* 33 (1996) 683.
- [4] C. Albrecht, J.H. Smet, D. Weiss, K. von Klitzing, et al., *Phys. Rev. Lett.* 86 (2001) 147.
- [5] P. Středa, *J. Phys. C* 15 (1982) L1299.
- [6] D.J. Thouless, M. Kohmoto, M.P. Nightingale, M. den Nijs, *Phys. Rev. Lett.* 49 (1982) 405.
- [7] R.B. Laughlin, *Phys. Rev. B* 23 (1981) 5632.
- [8] D. Springsguth, R. Ketzmerick, T. Geisel, *Phys. Rev. B* 56 (1997) 2036.